WORLD CONFERENCE ON TIMBER ENGINEERING 2025
BRISBANE, AUSTRALIA
Advancing Timber for the Future Built Environment

EXPERIMENTAL STUDY ON BRITTLE FAILURE OF LATERALLY LOADED STEEL-TO-CLT CONNECTIONS WITH INCLINED SELF-TAPPING SCREWS

Huiqi Wang[1], Lina Zhou[2], Ying-Hei Chui[3]

ABSTRACT: Self-tapping screws (STSs) are one of the most commonly used fasteners in modern mass timber construction. The new STS design provision in CSA O86-24 has not fully addressed the brittle failure of inclined STS connections due to a lack of research data. To fill this knowledge gap, a series of tests on steel-to-CLT connections with STSs at different insertion angles, penetration lengths and lateral load directions were conducted. The results reveal that plug-step shear is the dominant brittle failure mode in these connections, indicating the necessity to include the plug-step shear in the brittle failure modes in Canadian timber design standard. Based on the observed failure mechanisms, a new mechanics-based equation for plug-step shear was proposed with a modification factor to account for the uneven stress development and sequential failure mechanisms on different failure planes. The proposed new model with a modification factor of 0.65 is found to provide a better overall prediction in both accuracy and precision compared with the brittle failure model in CSA O86.

KEYWORDS: steel-to-CLT connection, brittle failure, lateral load, inclined self-tapping screw

1–INTRODUCTION AND BACKGROUND

The increasing use of mass timber products in modern construction has been largely driven by environmental awareness and policies of promoting sustainable and renewable materials [1]. Self-tapping screws (STSs) have gained great popularity in mass timber construction due to their high load-carrying capacity, ease of installation, and applicability in various connection configurations. Recognizing their growing usage and importance, the latest edition of the Canadian timber design code, CSA O86-24, has incorporated a new design provision for STS connections [2].

The new CSA O86-24 provision addresses both ductile and brittle failure modes for 90-degree STS connections under lateral loads [2]. The brittle failure resistance for partially penetrated STS connections with wood members is determined by the lowest resistance among four possible failure modes (Figure 1): plug shear (PS), step shear (SS), row shear (RS), and net tension (NT). The resistance of each brittle failure mode other than plug shear is calculated as the sum of the resistance of the corresponding failure planes, as illustrated in Figure 1. For plug shear resistance, the greater of the head tensile plane resistance plus the bottom shear and the side shear plane resistance is used for lumber, glulam, and mechanically laminated timber (MLT) while the sum of

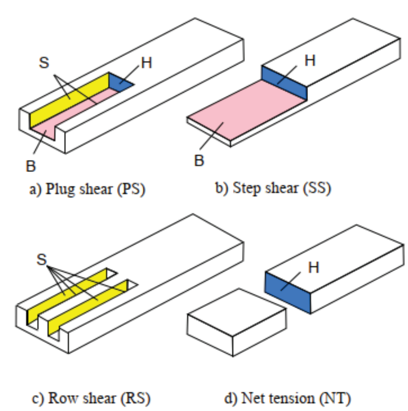

Figure 1. Failure modes and failure planes in CSA O86-24 (H: head tensile plane; S: Side shear plane; B: Bottom shear plane

[1] Huiqi Wang , Department of Civil Engineering, University of Victoria, Victoria, BC V8P 5C2, Canada, huiqi_wang@outlook.com
[2] Lina Zhou, Department of Civil Engineering, University of Victoria, Victoria, BC V8P 5C2, Canada, linazhou@uvic.ca
[3] Ying-Hei Chui, Department of Civil and Environmental Engineering, University of Alberta, Edmonton, AB T6G 1H9, Canada, yhc@ualberta.ca

https://doi.org/10.52202/080513-0239

all failure plane resistance is adopted for cross laminated timber (CLT) connections to account for the reinforcement obtained by the cross-layers. Although good agreement was observed between the test results and code prediction [3, 4], the failure modes in CSA O86-24 do not fully capture the actual failure mechanism of steel-to-CLT STS connections.

Research on CLT connections with 90-degree and 45-degree STSs has shown that it may exhibit a new brittle failure mode due to the cross-laminated layers [5-7], i.e., a mixed mode of plug shear in longitudinal layers with wood grain aligned parallel to the load and step shear in transverse layers with wood grain aligned perpendicular to the load, which we term "plug-step shear" thereafter in this paper. In CSA O86-24 [2], plug shear is characterized by continuous side shear planes that cut through the effective thickness irrespective of the grain direction (Figure 1 a)), whereas in plug-step shear discussed in this paper, the side shear planes only develop in longitudinal layers.

For inclined STS connections, there are currently limited design guidelines for the brittle failure resistance in CSA O86-24 Clause 12.12.10.2 [2] notes that the brittle failure of inclined STS connections may be designed analogously to that of 90-degree STS connections. Further research is needed to validate this approach and evaluate the necessity of adding plug-step shear as one of the possible brittle failure modes in design.

In this study, a series of STS connection tests were performed to investigate the brittle failure behaviour of steel-to-CLT connections with inclined self-tapping screws. 90-degree STS connections were also tested as a reference. The primary objective of this study was to investigate the brittle failure behaviour of steel-to-CLT connections with inclined STSs, specifically the resistance of plug-step shear failure, and to develop predictive equations for this failure mode.

2–STEEL-TO-CLT STS CONNECTION TEST

2.1 SPECIMEN CONFIGURATIONS

The specimens tested in this project were designed to fail in either step shear or plug-step shear, which were anticipated to be the dominant brittle failure modes in steel-to-CLT STS connections. The key parameters analyzed included STS insertion angle (45° and 90°), penetration depth (two and three layers), and CLT panel width (narrow: 130 mm and wide: 390 mm). Figure 2 shows the dimensions of a specimen.

It is challenging to achieve the brittle failure modes following the minimum spacing requirements in CSA O86 [2] based on pre-test calculation. Therefore, screw spacing and end distances were reduced below the minimum spacing requirements and staggered STSs were added to achieve the occurrence of brittle failure modes. For all the connections tested in this study, S_P = 40 mm, S_Q = 28 mm and a_L= 40 mm as shown in Figure 2. The specimens were designed as an unsymmetrical configuration, where screws were installed only on one side of the CLT panel.

All CLT panels used in this study consist of five laminates with a total thickness of 175 mm and length of 700 mm. The panels were stored in an environmental chamber at 21°C and 65% relative humidity for over one month before STS installation. The STSs used in the tests were VGS 11 × 80 mm, VGS 11 × 125 mm, and VGS 11 × 175 mm, supplied by Rothoblaas. These screws are fully threaded with countersunk heads, commonly used for inclined STS connections. Predrilled holes were created in the CLT panels using a 6.35 mm (1/4") drill bit, which is the closest available size to the 7 mm diameter recommended in the supplier's manual. The steel plates used in the tests were 12.5 mm (1/2") thick, made from Grade 300W steel or better.

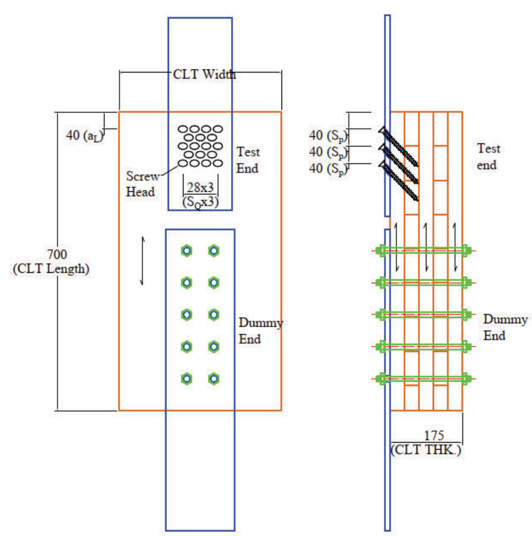

Figure 2. Specimen dimensions

https://doi.org/10.52202/080513-0239

Table 1 Configurations of STS Connections

Group	Penetration Layers	Screw diameter × length (mm × mm)	Load Direction	Angle	CLT width (mm)	Fasteners	Staggered fasteners
C11×125S4×3N45P2	2	11 × 125	Parallel	45◦	130	4 × 3	3 × 2
C11×125S4×3W45P2	2	11 × 125	Parallel	45◦	390	4 × 3	3 × 2
C11×80S4×3N90P2	2	11 × 80	Parallel	90◦	130	4 × 3	3 × 2
C11×80S4×3W90P2	2	11 × 80	Parallel	90◦	390	4 × 3	3 × 2
C11×175S4×4N45P3	3	11 × 175	Parallel	45◦	130	4 × 4	3 × 3
C11×175S4×4W45P3	3	11 × 175	Parallel	45◦	390	4 × 4	3 × 3
C11×125S4×4N90P3	3	11 × 125	Parallel	90◦	130	4 × 4	3 × 3
C11×125S4×4W90P3	3	11 × 125	Parallel	90◦	390	4 × 4	3 × 3

Table 1 presents configurations of STS connections tested in this study. The specimens were labelled based on configurations (Table 1). For example, in C11×125S4×3W45P2, 'C' represents CLT; '11×125' denotes the diameter (11 mm) and length (125 mm) of the STSs; 'S' indicates self-tapping screws; '4×3' describes the STS pattern with four rows and three columns; 'W' signifies wide CLT panels (390 mm), while 'N' represents narrow panels (130 mm); '45' refers to the STS insertion angle; 'P' denotes loading parallel to the major strength direction of CLT panels; '2' indicates penetration into two layers; and the final digit ('1') represents the replicate number. Three replicates were tested per configuration. There were 24 specimens in total tested and reported in this paper.

2.2 EXPERIMENTAL SETUP

The tests were conducted in the Structures Laboratory at the University of Victoria. Figure 3 illustrates the experimental setup. The specimen was mounted in a universal testing machine (UTM), with two hydraulic grips securing two steel plates—one attached on the test end and the other on the dummy end. Two linear variable differential transformers (LVDTs) were attached to the steel plate at the test end and the reference point was attached to CLT panels to record relative movement. The displacement loading rate was set at 2.5 mm/min, and testing was terminated once the applied load dropped to below 80% of the recorded peak load. To prevent premature failure in the dummy end, 5/8" bolts were used (Figure 3), ensuring a higher load-carrying capacity than the test end.

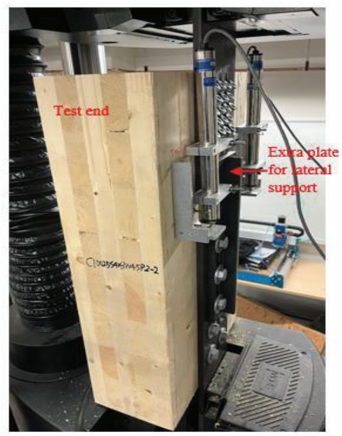

Figure 3. Test setup (C11×125S4×3W45P2-2, test end is positioned at the top)

3–RESULTS

3.1 PEAK LOAD AND LOAD-DISPLACEMENT CURVES

Table 2 presents the peak loads of the test specimens. All the specimens failed in plug-step shear. For wide CLT specimens, the resistance of connections with 45-degree STSs penetrating two and three layers of CLT panels is 32% and 43% higher than that of 90-degree STS connections respectively, while for narrow CLT samples, the capacity of 45-degree and 90-degree STS connections are almost identical. The resistance of wide CLT connections is higher than that of narrow CLT connections, ranging from 23% to 103%. This difference is more significant for samples with 45-degree STSs compared to 90-degree STSs and STSs penetrating three layers compared to two layers.

https://doi.org/10.52202/080513-0239

Table 2 Summary of The Peak Load

Group	Peak load (kN)			Avg. Peak load (kN)
	Rep 1	Rep 2	Rep 3	
C11×125S4×3N45P2	82	100	92	92
C11×125S4×3W45P2	169	155	124	150
C11×80S4×3N90P2	97	76	106	93
C11×80S4×3W90P2	105	126	112	114
C11×175S4×4N45P3	79	100	105	94
C11×175S4×4W45P3	192	201	181	191
C11×125S4×4N90P3	72	106	105	94
C11×125S4×4W90P3	152	125	125	134

The load-displacement curves of test specimens are presented in Figure 4. For C11×125S4×4W90P3 (Figure 4 d)), there is a secondary increase surpassing the first peak in the load-displacement curve following the initial brittle failure. This behaviour was attributed to the onset of yielding in STSs, which allowed load redistribution and resistance recovery in the connection. The peak loads in Table 2 correspond to the first peak of brittle failure. All specimens exhibited brittle failure, as evidenced by a sudden drop in load resistance.

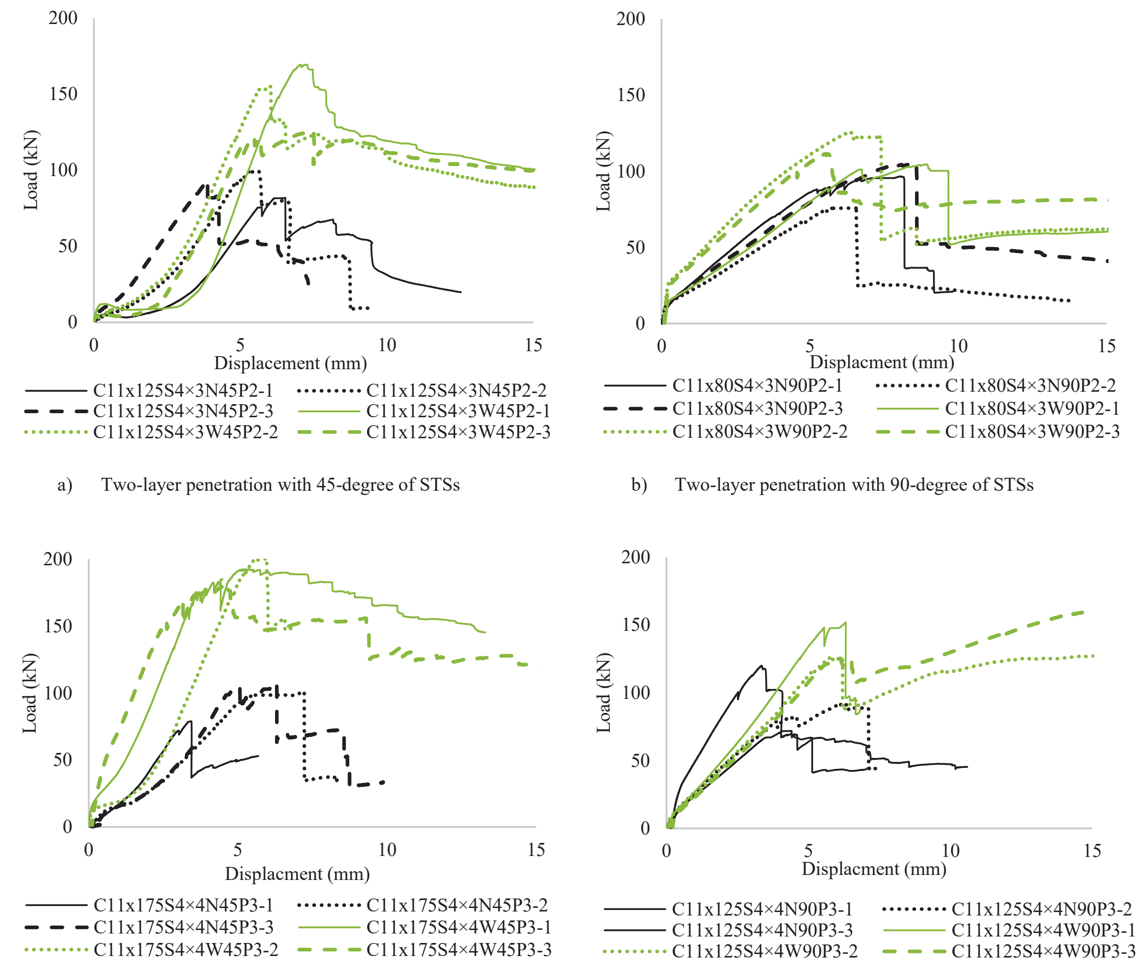

a) Two-layer penetration with 45-degree of STSs

b) Two-layer penetration with 90-degree of STSs

c) Three-layer penetration with 45-degree of STSs

d) Two-layer penetration with 90-degree of STSs

Figure 4 Comparison of load-displacement curves of STS connections with narrow (black) and wide (green) CLT panels

https://doi.org/10.52202/080513-0239

3.2 FAILURE MODES AND EFFECTIVE DEPTH

The primary failure mode observed in this study is plug-step shear (Figure 5). There was no pure plug shear as defined in CSA O86-24 observed in these tests as the transverse CLT layers usually failed in splitting instead of shear perpendicular to the grain. The plug-step shear failure mechanism involves three types of failure planes as summarised in Figure 6: the side shear planes of parallel layers (yellow), the head tensile plane of parallel layers (blue) and the bottom and top shear planes (red). The current equations in CSA O86-24 for a CLT panel connection assume that all failure planes reach their peak resistance simultaneously and the resistance of a connection is determined as the sum of the resistance of all failure planes. However, experimental observations from this study indicate that this assumption is not always valid. In contrast, the failure planes on different CLT layers and with different failure mechanisms showed sequential failure phenomenon (Figure 7) and usually the planes closer to the steel plate experienced larger displacements and reached their peak resistance prior to the others. Similar findings have been reported by other researchers [4].

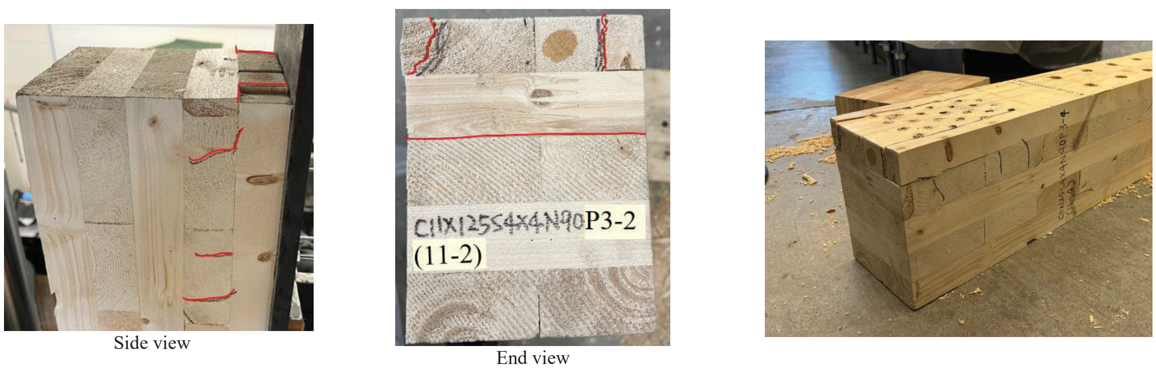

a) Plug-step shear failure in narrow samples (C11×125S4×4N90P3-2)

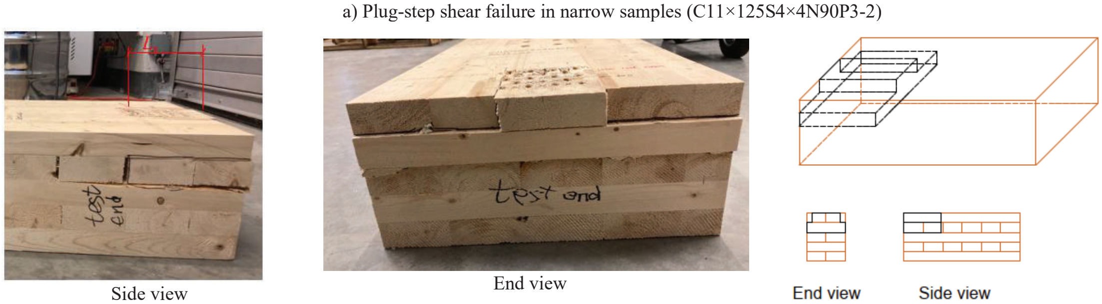

b) Plug-step shear failure in wide samples pentrating into two layers (C11×125S4×3W45P2-1)

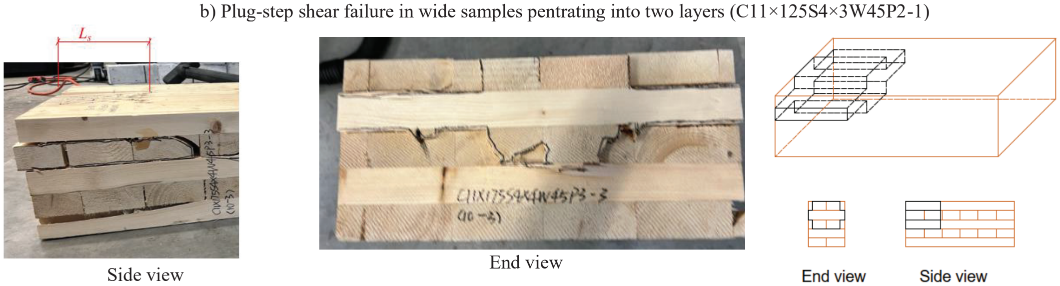

c) Plug-step shear failure in wide samples penetrating into three layers (C11×175S4×4W45P3-3)

Figure 5 Failure of steel-to-CLT STS connections loaded parallel to the CLT major strength direction

https://doi.org/10.52202/080513-0239

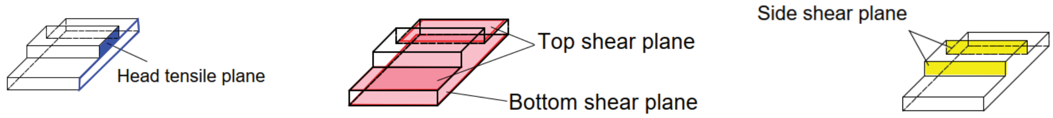

a) Connection loaded parallel to the major strength direction with STS penetrating into two layers

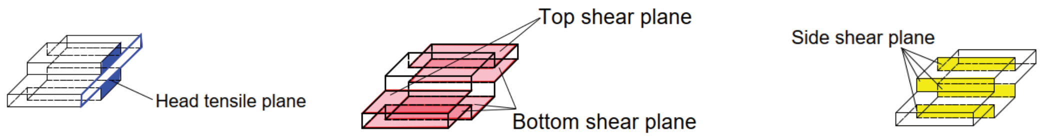

b) Connection loaded parallel to the major strength direction with STS penetrating into three layers

Figure 6. Failure planes in plug-step shear failure mode

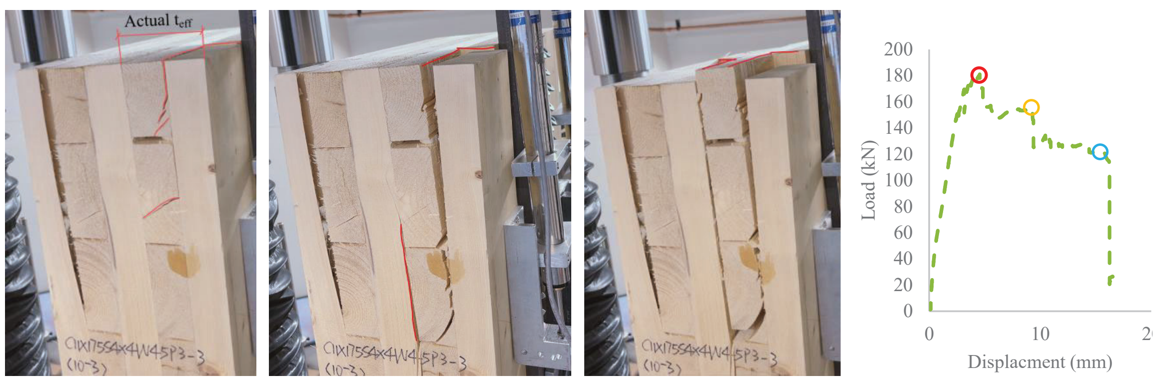

(a) The 1st layer was pulled out in plug shear while the 2nd and 3rd layers were still held together at the peak load. (red point in c))

(b) Following the first peak, the rolling shear plane between the 2nd and 3rd layer was developed (orange point in c))

(c) With further increased displacement, the 2nd and 3rd layers were pulled out finally, causing a significant drop in the measured load (blue point in c))

(d) Load-displacement curve of C11×175S4×4W45P3-3

Figure 7 Sequence failure of C11×175S3×4W45P3-3

Effective depth, t_{eff}, is one of the key parameters in calculating the brittle failure resistance in CSA O86-24 as it defines the depth of the failure block (Figure 8 a)). The equation provided for partially penetrated wood member in CSA O86-24 Clause 12.12.10.7.11 [2] was developed based on the analytical results of a beam-on-elastic-foundation model with 90-degree dowel-type fasteners [6-7]. Table 3 compares the calculated effective depth according to CSA O86-24, the actual effective depth observed in tests and the penetration depth. For inclined STSs, the projected depth along the thickness of CLT panels was used as the penetration depth to calculate the effective thickness. The actual effective depth in this study was measured at the 1st peak drop down as shown in Figure 7 a) and d). The failure on other layers of CLT panels may not be observed at that moment. It can be seen from Table 3 that the effective depth calculated using CSA O86-24 aligns well with the actual effective thickness with an average ratio of 1.07.

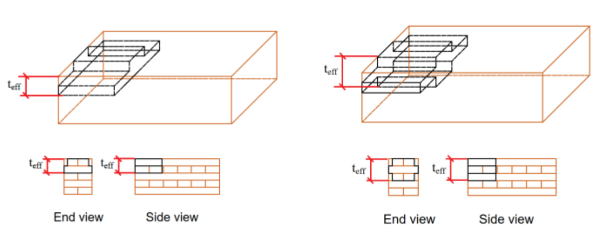

a) Effective depth, t_{eff}, in plug-step shear

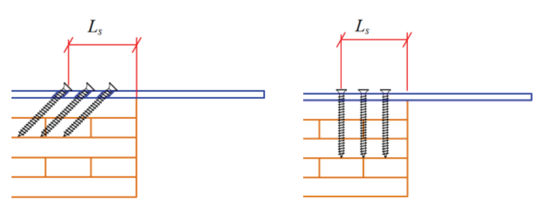

b) Critical length, L_S, in plug-step shear

https://doi.org/10.52202/080513-0239

Figure 8 Effective depth and critical length in plug-step shear

Table 3 Comparison of calculated and actual effective depth

Group	Average actual t_{eff} (mm)	Cal. t_{eff} (mm)	Penetration depth (mm)	Cal. t_{eff} / Actual t_{eff}	Pentrartion / Actual t_{eff}
C11×125S4×3N45P2	68	52	69	0.76	1.01
C11×125S4×3W45P2	35	52	69	1.49	1.96
C11×80S4×3N90P2	59	49	57	0.83	0.97
C11×80S4×3W90P2	35	49	57	1.39	1.63
C11×175S4×4N45P3	48	57	97	1.19	2.00
C11×175S4×4W45P3	59	57	97	0.97	1.64
C11×125S4×4N90P3	70	57	92	0.81	1.31
C11×125S4×4W90P3	50	57	92	1.13	1.84
			Average:	1.07	1.55

3.3 PROPOSED MODEL FOR PLUG-STEP SHEAR FAILURE

Failure Plane Resistance

The resistance of each failure plane is calculated following the provisions in CSA O86-24 Clause 12.12.10.7 [2] with the critical area for plug-step shear proposed in this study (Figure 6).

- Side shear plane

The side shear plane resistance, $PB_{s,//}$, is defined as:

$$PB_{s,//} = 1.5\, f_v\, (t_{eff} - t_{\perp})\, L_s \qquad (1)$$

where f_v is the longitudinal shear strength of wood member; t_{eff} is the effective thickness defined as CSA O86-24 [2] clause 12.12.10.7.11 with projected bearing length used as t_i for partially penetrated wood member with inclined STS; $t_{\perp}$ is the projected penetrated depth in CLT transverse layer with wood grain aligned perpendicular to the load; and L_s is the critical length defined as the length from the loading end to the centre of the head of first row STSs (Figure 8 b)).

- Head tensile plane

The head tensile resistance of the layers perpendicular to the load is conservatively excluded. The resistance of the head tensile plane of the CLT member, $PB_{t,//}$, is defined as:

$$PB_{t,//} = 1.25\, f_t\, (n_R - 1)\, S_Q\, (t_{eff} - t_{\perp}) \qquad (2)$$

where f_t is the tension strength parallel to the grain; n_R is the number of fastener rows; S_Q is the fastener spacing perpendicular to the load direction measured from the head of the STSs.

- Bottom and top shear planes

The bottom and top shear plane resistance is defined as:

$$PB_{sb} = 0.75 f_s \sum A_{P,si} \qquad (3)$$

where f_s is the rolling shear strength; and $A_{P,si}$ is the critical of the rolling shear planes in laminate i which is defined as:

a) for top shear planes:

$$A_{P,si} = (b - (n_R - 1)\, S_Q)\, L_s \qquad (4)$$

where b is the width of the CLT panel.

b) for bottom shear planes:

$$A_{P,sn} = b\, L_s \qquad (5)$$

It was observed that the bottom and top shear planes might fail in either longitudinal shear or rolling shear(Figure 5 c). Therefore, rolling shear strength is conservatively used for all the top and bottom shear planes.

Connection Resistance

To account for the uneven stress distribution in steel-to-CLT STS connections, a modification factor of 0.65 is applied to modify the total plug-step shear resistance. This coefficient was originally used in bolt connection design provisions to adjust the resistance where a wood side member is loaded on one surface based on the work of Mohammad and Quenneville [10]. The STS connection resistance for plug-step shear failure, PPS_{rT}, is defined as:

$$PPS_{rT} = 0.65(PB_{s,//} + PB_{t,//} + PB_{sb}) \qquad (6)$$

Comparison with the test results

Mean material properties cited from Canadian Lumber Properties report [11] were used as input to calculate the predicted resistance, F_{Pi}, for different model, which is considered to be more reliable in model performance assessment [12]. The predicted resistance based on the brittle failure model for STS connections in CSA O86-24 (Model 1), F_{P1}, the proposed model of plug-step shear without modification factor (Model 2), $F_{P2,}$ and the plug-step shear model with a modification factor of 0.65 (Model 3), $F_{P3,}$ are compared with the test resistance, $F_{T,}$ from this study (Table 4). Table 5 summarizes the difference among the three prediction models. A boxplot of F_{Pi} / F_T (Figure 9) provides a direct comparison of the three models' accuracy, where the average and median are indicated by a cross and a line in the box, respectively. Figure 10 presents a comparison between F_T (x-axis), and F_P (y-axis), for the three models. A linear regression fit passing through the origin is included with the corresponding slope (m) and coefficient of determination (R^2). The dashed line represents the ideal prediction ratio of $F_P/F_T = 1$.

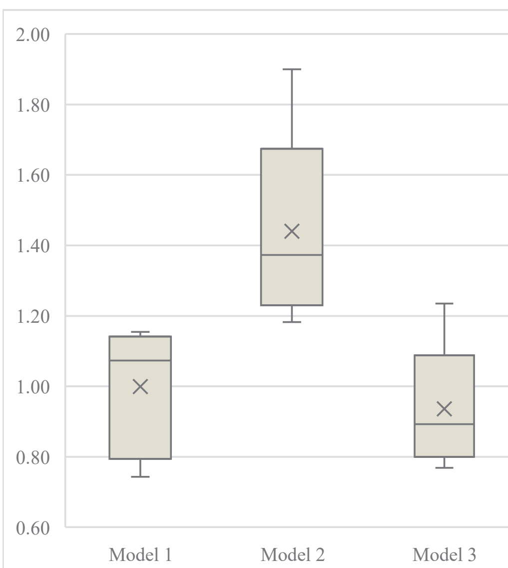

Figure 9 Boxplot of F_{Pi} / F_T

Figures 9 and 10 show that the plug-step shear model without modification factor (Model 2) exhibits the least accuracy, significantly overestimating the test results, with F_{Pi} / F_T consistently larger than 1 (Figure 9) and *m* notably greater than 1 (Figure 10). This overprediction aligns with test observations, which indicated that the stress distribution on failure planes was not uniform, and the maximum capacity of these planes was not reached simultaneously (Figure 7). Both CSA O86-24 (Model 1) and plug-step model with a modification factor of 0.65 (Model 3) give a close prediction to test resistance. Table 4 shows the comparison of the model prediction to test resistance. It can be seen that, Model 1 overestimates the resistance of five groups of connections while Model 3 gives a more reliable prediction, overestimating two groups of connections with a smaller scatter as shown in Figure 9. Additionally, Model 1 does not capture the actual failure mechanism of the connections. According to Model 1, a steel-to-CLT fails in plug shear or step shear (Table 4). Overal, Model 3 captures the actual failure mode of steel-to-CLT connections with a prediction/test ratio closest to 1 (0.943) and the highest R^2 value of 0.975.

Table 5 Three prediction models

Model	Details
1	Follow the CSA O86-24 Clause 12.12.10.7 [2] for both 45-degree and 90-degree STS connections. Four possible failure modes are considered: plug shear, step shear, row shear, and net tension.
2	Follow the proposed plug-step shear model and consider plug-step shear failure only without modification factor
3	Follow the proposed plug-step shear model and consider plug-step shear failure only with a modification factor of 0.65

Table 4 Comparison of prediction models to test resistance

Group	Test	Model 1			Model 2		Model 3	
	F_T (kN)	F_{P1} (kN)	Mode	F_{P1} / F_T	F_{P1} (kN)	F_{P2} / F_T	F_{P3} (kN)	F_{P3} / F_T
C11×125S4×3N45P2	92	101	Step shear	1.11	110	1.20	71	0.78
C11×125S4×3W45P2	150	111	Plug shear	0.74	201	1.35	131	0.87
C11×80S4×3N90P2	93	101	Step shear	1.09	110	1.18	71	0.77
C11×80S4×3W90P2	114	108	Plug shear	0.95	201	1.76	131	1.15
C11×175S4×4N45P3	94	109	Step shear	1.15	132	1.40	86	0.91
C11×175S4×4W45P3	191	142	Plug shear	0.74	255	1.33	165	0.86
C11×125S4×4N90P3	94	109	Step shear	1.15	132	1.40	86	0.91
C11×125S4×4W90P3	134	141	Plug shear	1.05	255	1.90	165	1.23

https://doi.org/10.52202/080513-0239

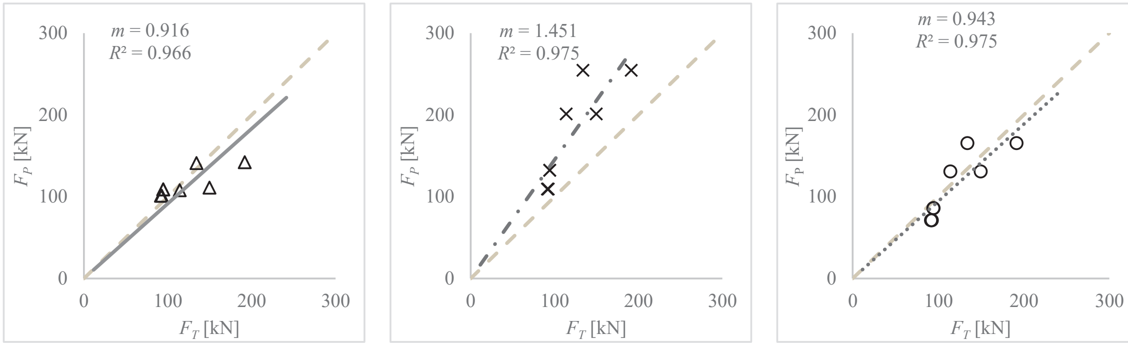

(a) Model 1 (b) Model 2 (c) Model 3

Figure 10 Comparison of STS connection resistance obtained from the tests and the theoretical prediction

4–CONCLUSION

A series of tests on steel-to-CLT connections with inclined STSs were conducted to study their brittle failure modes. Connections with 90-degree STSs were also tested as a reference. The results show that plug-step shear is the primary brittle failure mode in steel-to-CLT STS connections. The pure plug shear failure mode observed in STS connections with other mass timber products such as glulam members, does not occur in CLT connections. Based on the observed failure mechanism, a new failure model of plug-step shear was proposed in this study.

The plug-step model with (Model 3) and without (Model 2) a modification factor, and the brittle failure model for STS connections in CSA O86-24 (Model 1) are compared with test resistance. Results show that the plug-step model with a modification factor of 0.65 (Model 3) provides the best prediction to the test resistance and reflects the actual failure mechanism for steel-to-CLT STS connections. While the CSA O86-24 model provides statistically reasonable precision, it shows a weak overall prediction in accuracy as it does not capture the actual failure mechanisms of the connections.

Future research may focus on getting a better understanding on the resistance contribution of each failure plane. A refined model that can more accurately represent the roles of different failure planes may be necessary.

5–ACKNOWLEDGEMENT

The authors would like to thank BC Forestry Innovation Investment Ltd. for funding support of this research (Project # 24/25-UVIC-ISS-W25-048).

6–REFERENCES

[1] M. Yurrita and J. M. Cabrero. "New design model for brittle failure in the parallel-to-grain direction of timber connections with large diameter fasteners." In: Engineering Structures 217 (2020), p. 110557. doi: 10.1016/j.engstruct.2020.110557.

[2] CSA O86:24. *Engineering design in wood*. Toronto, ON, Canada, 2024.

[3] C. Ni and J. Niederwestberg. "Investigation of brittle failure modes in self-tapping screw steel-to-wood connections parallel to the grain – Part I." In: *FPInnovations Report*, Vancouver, B.C., Canada, 2022.

[4] C. Ni and J. Niederwestberg. "Investigation of brittle failure modes in self-tapping screw steel-to-wood connections parallel to the grain – Part II." In: *FPInnovations Report*, Vancouver, B.C., Canada, 2022.

[5] B. Azinović, J. M. Cabrero, H. Danielsson, and T. Pazlar. "Brittle failure of laterally loaded self-tapping screw connections for cross-laminated timber structures." In: *Engineering Structures* 266 (2022), p. 114556.

[6] P. Zarnani and P. Quenneville. "New design approach for controlling brittle failure modes of small-dowel-type connections in cross-laminated timber (CLT)." In: *Construction and Building Materials* 100 (2015), pp. 172–182.

[7] H. Wang, L. Zhou, and Y. H. Chui, 'Experimental study of brittle failure of cross laminated timber (CLT) connections with inclined self-tapping screws', presented at *NHICE-04* (2024).

[8] J. M. Cabrero, N. López Rodríguez, T. Tannert, A. Salenikovich, and Y. H. Chui. "Brittle failure modes of connections with dowel-type fasteners loaded parallel to the grain: A comparison between Eurocode 5 and CSA O86." In: *INTER 2024*, Paper 58-7-9 (2024).

[9] M. Yurrita and J. M. Cabrero. "Effective thickness of timber elements for the evaluation of brittle failure in timber-to-steel connections with large diameter fasteners loaded parallel-to-grain at the elastic range: A new method based on a beam on elastic foundation." In: *Engineering Structures* 209 (2020), p. 109959.

[10] M. Mohammad and J. H. Quenneville. "Bolted wood-steel and wood-steel-wood connections: verification of a new design approach." In: *Canadian Journal of Civil Engineering* 28.2 (2001), pp. 254–263.

[11] J. D. Barrett and W. Lau. *Canadian Lumber Properties.* 1994th ed. Canadian Wood Council.

[12] J. M. Cabrero and M. Yurrita. "Performance assessment of existing models to predict brittle failure modes of steel-to-timber connections loaded parallel-to-grain with dowel-type fasteners." In: *Engineering Structures* 171 (2018), pp. 895–910.

https://doi.org/10.52202/080513-0239